New materials for high-efficiency spin-polarized electron source

A. Janotti

Metals and Ceramics Division, Oak Ridge National Laboratory, TN

In Collaboration with S.-H. Wei, *National Renewable Energy Laboratory, CO*

Work supported by Basic Energy Sciences- DOE

Outline

• Generating spin-polarized electrons from semiconductors using near-band-edge photo-excitation

•GaAs, GaAsP, and SL's as SPES
•CuPt-ordered semiconductor alloys
•Chalcopyrites I-III-VI_2 and II-IV-V_2

•How to improve the spin polarization

•CuAu-ordered $AgGaSe_2$ as an high quality spin-polarized electron source

High-quality spin-polarized electron source

- High spin polarization
- High quantum efficiency
- High Reliability

Applications:

- Atomic physics
- Condensed-matter physics
- Nuclear physics
- High-energy particle physics

Seminal Works: GaAs as SPES (1976)

Photoemission of spin-polarized electron from GaAs
Pierce, D.T. & Meier, F. Physical Review B **13**, 5484 (1976).
Laboratorium für Festkörperphysik, Eidgenössische Technische Hochschule, CH 8049, Zürich, Switzerland

Source of Spin-Polarized Electrons from GaAs
Pierce, D.T. , Meier, F. & Siegmann U.S. Patent 3,968,376, issued July 6, 1976.

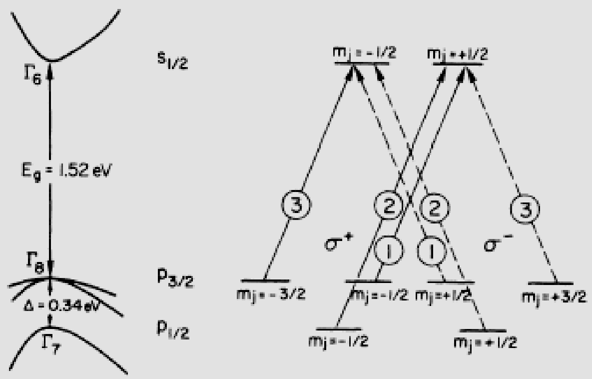

FIG. 2. On the left, an E-vs-k diagram of the energy bands of GaAs near $k = 0$ shows the energy gap E_g and the spin-orbit splitting Δ of the valence bands. The degenerate states at $k = 0$ are labeled on the right by their m_J quantum numbers. The allowed transitions for σ^+ ($\Delta m_j = 1$) and σ^- ($\Delta m_j = -1$) circularly polarized light are shown by the solid and dashed lines, respectively. The circles numbers represent the relative transition probabilities.

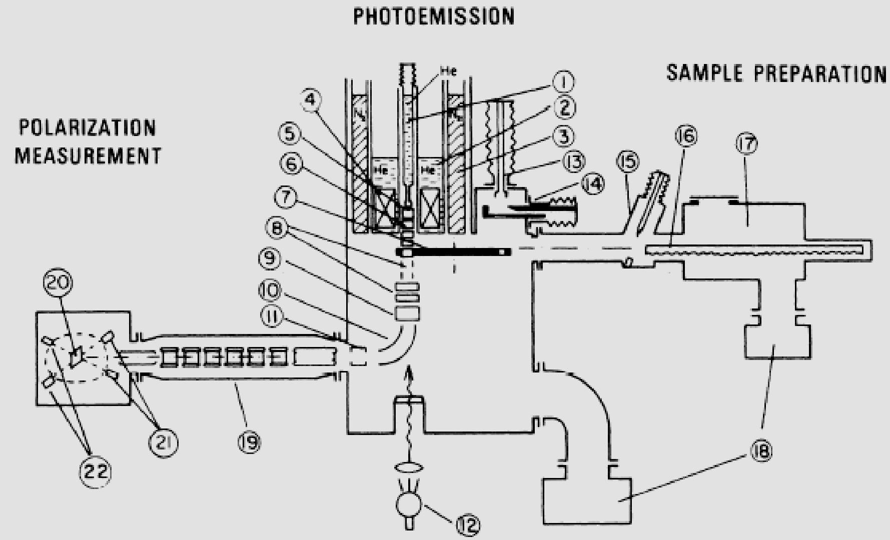

FIG. 4. Schematic diagram of the apparatus: 1, Movable He cryostat with sample gripper; 2, He cryostat; 3, liquid nitrogen; 4, superconducting coil; 5, sample in measuring position; 6, accelerating electrodes; 7, rotatable wheel with samples; 8, parallel beam shifters; 9, plane condenser; 10, cylindrical condenser; 11, aperture; 12, light source; 13, gripper for cleaving; 14, cleaving mechanism; 15, ultrahigh-vacuum valve; 16, rack-and-pinion linear motion; 17, sample preparation chamber; 18, ion-getter pumps; 19, seven-stage accelerator; 20, gold foil; 21, detectors to measure Mott asymmetry; 22, forward detectors to monitor beam.

GaAs as SPES revolutionized the study of spin-dependent phenomena

Spin-orbit interaction
Interaction of the spin of the electron with its own orbital angular momentum
Polarized electron scattering from a W(100) surface

Exchange interaction
Consequence of Pauli principle
Surface Magnetization of Ferromagnetic Ni(110)

GaAs as SPES revolutionized the study of spin-dependent phenomena

Spin-orbit interaction

Interaction of the spin of the electron with its own orbital angular momentum

Polarized electron scattering from a W(100) surface

Phys. Rev. Lett. ***42,*** *1349 (1979)*

Symmetry in Low-Energy-Polarized-Electron Diffraction

G. -C. Wang, B. I. Dunlap, R. J. Celotta, and D. T. Pierce

National Bureau of Standards, Washington, D. C. 20234

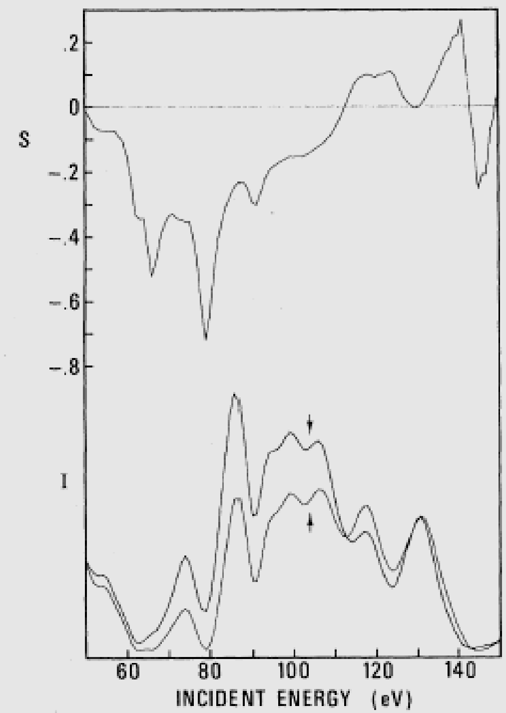

FIG. 2. The spin dependence of the scattering $S(E, \theta)$ is plotted for specular diffraction from W(100) at an angle of incidence of 15°. The scattered intensities resulting from an incident beam consisting of only spin up (↑) or of only spin down (↓) electrons are shown as $I_\uparrow$ and $I_\downarrow$.

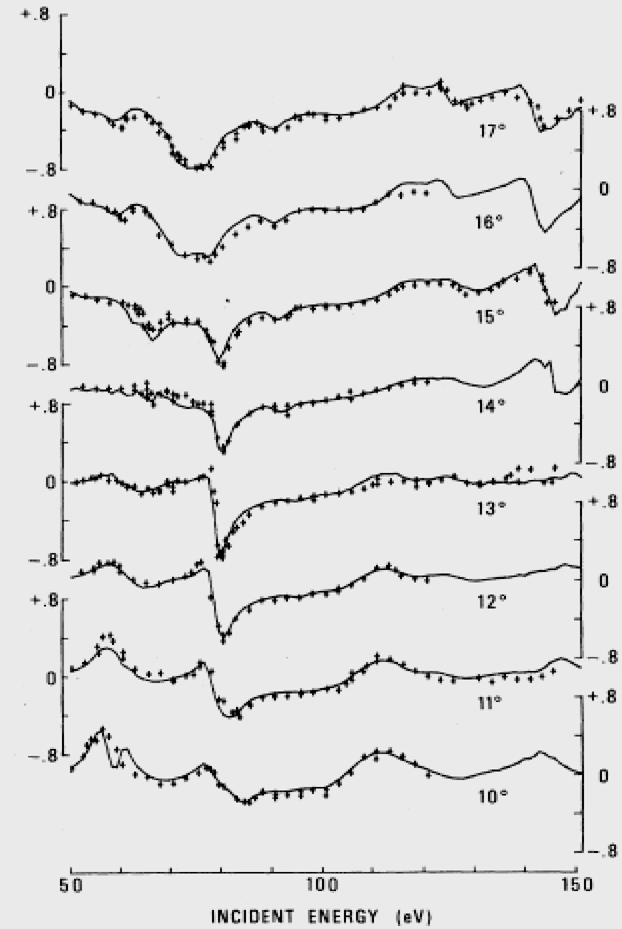

FIG. 3. Our measurements of $S(E, \theta)$ (solid line) are compared to the measurements $P(E, \theta)$ (crosses) of Ref. 2 of the (00) beam for angles of incidence from 10° to 17°. The scattering plane is in a (010) plane of the crystal. The curves are normalized as described in the text.

GaAs as SPES revolutionized the study of spin-dependent phenomena

Exchange interaction
Consequence of Pauli principle

Phys. Rev. Lett. ***43,*** *728 (1978)*

Surface Magnetization of Ferromagnetic Ni(110): A Polarized Low-Energy Electron Diffraction Experiment

R. J. Celotta, D. T. Pierce, and G. -C. Wang
National Bureau of Standards, Washington, D. C. 20234
S. D. Bader and G. P. Felcher
Argonne National Laboratory, Argonne, Illinois 60439

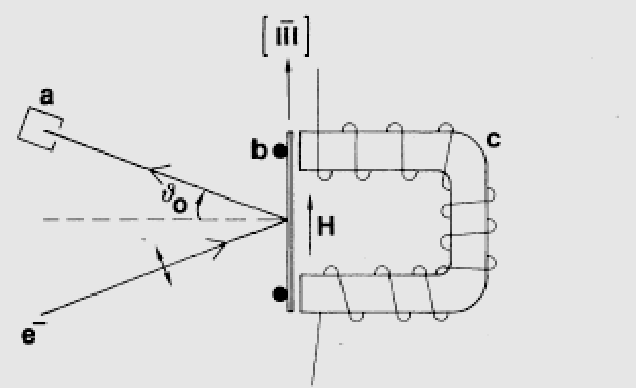

FIG. 1. The electron beam at an angle of incidence ϑ_0 is diffracted from the Ni(110) crystal into the Faraday cup (*a*). Ta rods (*b*) support the crystal which closes the magnetic circuit of the miniature electromagnet (*c*). The incident-electron spin polarization and the crystal magnetization lie in the scattering plane.

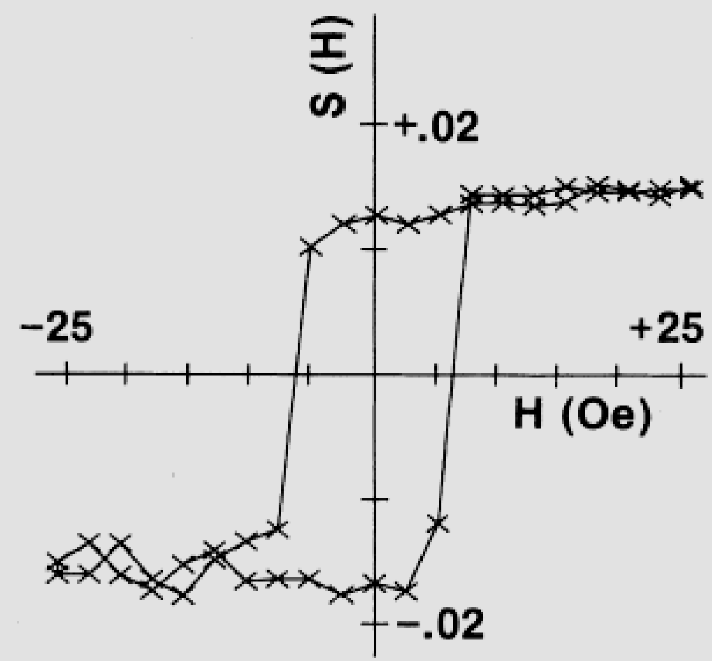

FIG. 2. A hysteresis curve, $S(H)$, at E= 125 eV and ϑ_0= 12°. The raw data points, which are connected by straight lines, were obtained between the $S(T)$ measurements (× and +) of Fig. 3.

Although GaAs is an efficient photoemitter, the maximum spin polarization of the emitted electrons
is limited to 50%.

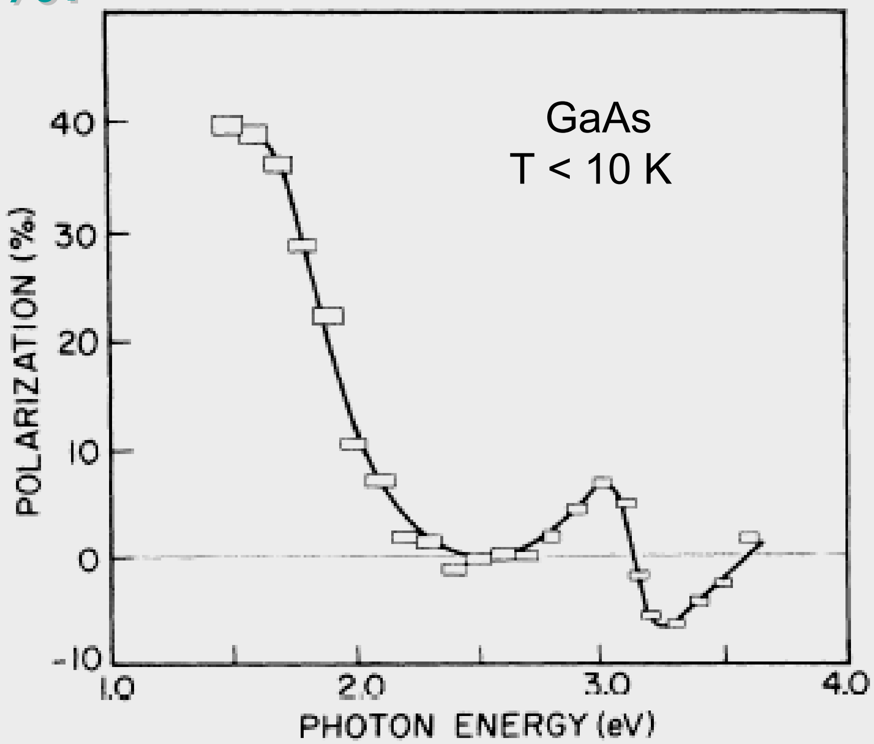

FIG. 6. Spectrum of spin polarization from GaAs + CsOCs at $T \leq 10$ K [the same sample and conditions as curve (a) of Fig. 5]. Note the high value of $P = 40\%$ at threshold ($\hbar\omega \sim 1.5$ eV) and positive and negative peaks at $\hbar\omega = 3.0$ and 3.2 eV.

Nowadays, most of the sources are *still* based on GaAs and related materials

Polarized Gas Targets and Polarized Beams,
7^{th} International Workshop, Urbana, IL 1997

Many important research institutes have a significant amount of the approved scientific projects based on polarized electron beams, and many of these experiments require high polarization (~80%).

SLAC in Stanford, CA - USA

Jefferson Lab. in Newport News, VA - USA

NIKHEF in Amsterdam, Netherlands

MIT-Bates in Middleton, MA –USA

MAMI in Mainz, Germany

- Generating spin-polarized electrons from semiconductors using near-band-edge photo-excitation

Schematic diagram of near-gap optical transition for circularly polarized light

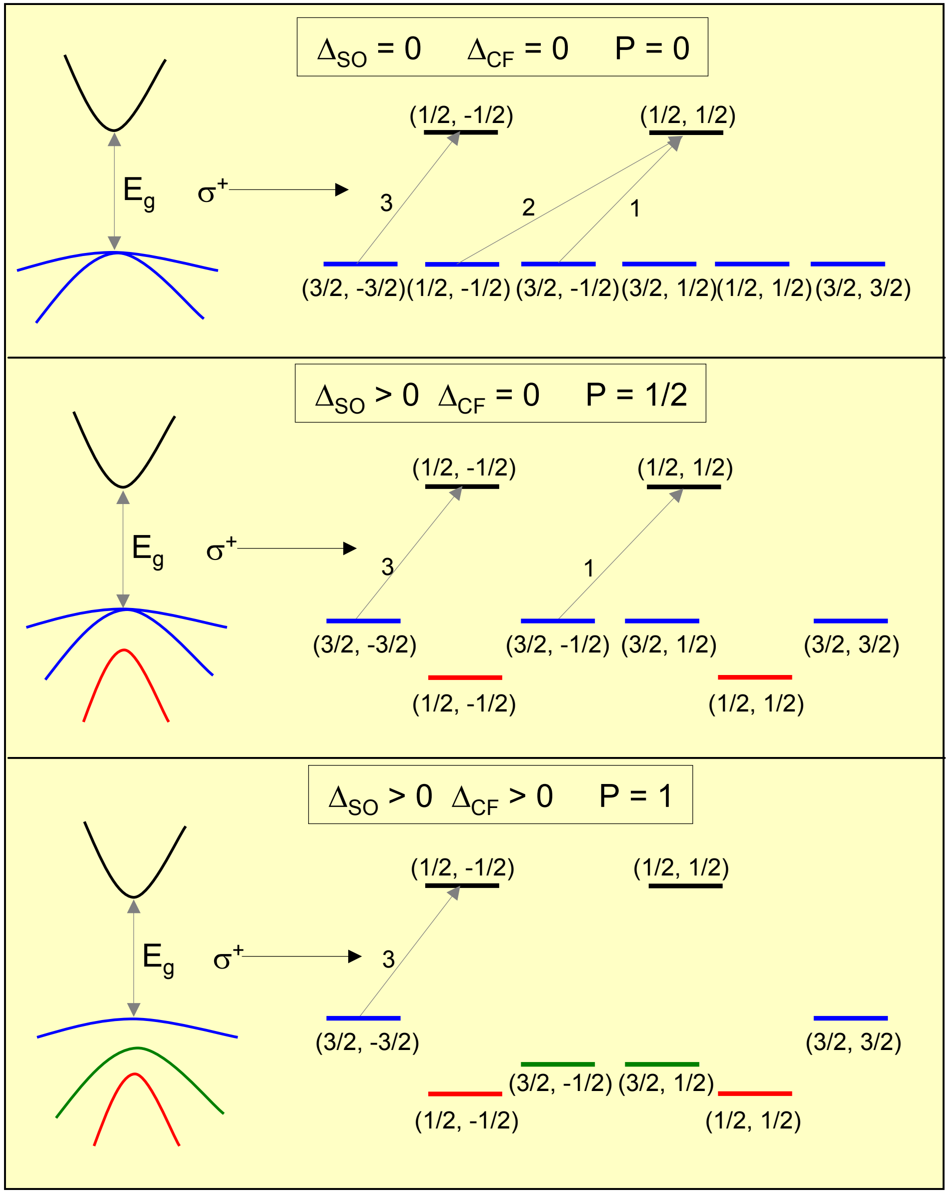

$$P = \frac{\left| I\downarrow - I\uparrow \right|}{\left| I\downarrow + I\uparrow \right|}$$

$$I = \left| \left\langle \Psi_f \left| H_{\text{int}} \right| \Psi_i \right\rangle \right|^2$$

$$H_{\text{int}} = X + iY$$ for σ^+ light

Ideal material for SPES application

- Direct band gap
- Large spin-orbit splitting
- Large and positive crystal field splitting

Collecting the spin-polarized electrons

"The art of activating GaAs photocatodes"

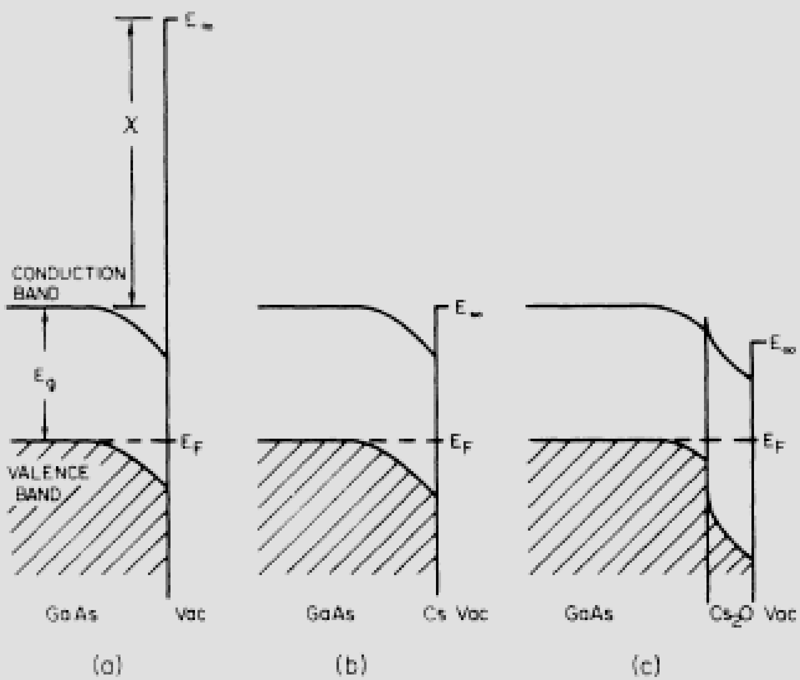

FIG. 3. Energy bands near the surface (E vs z) in p-type GaAs with different surface treatments: (a) clean GaAs with a high electron affinity; (b) GaAs with a layer of Cs, leading to an approximately zero electron affinity; and (c) GaAs with Cs–O treatment to produce a negative electron affinity.

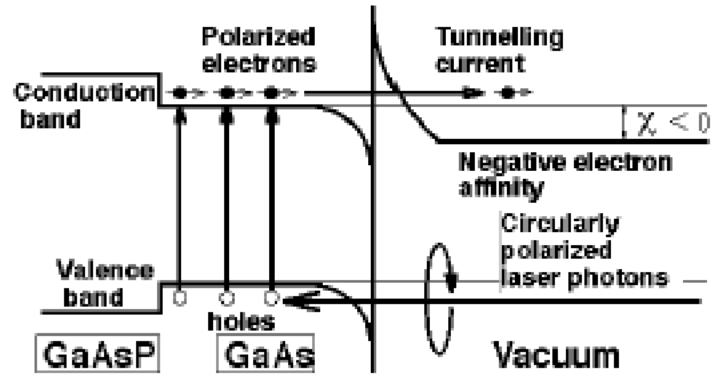

Fig. 1 : Principle of Strained GaAs-type PES

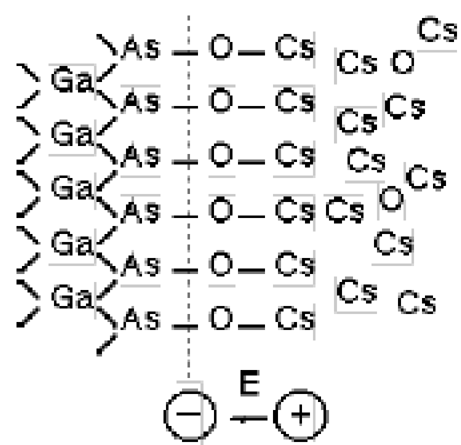

Fig. 2 : Microscopic view of NEA surface

Negative electron affinity condition

Ideal material for SPES application

- Direct band gap

- Large spin-orbit splitting

- Large and positive crystal field splitting

Substantial effort have been made to break GaAs 50% polarization limit

Strained materials

- GaAsP grown on GaAs
- GaAs grown on InGaAs
- GaAsP/GaAs superlattice
- CuPt-ordered GaAsP and InGaAs alloys

Chalcopyrites

- I-III-VI_2 $CuInSe_2$, $CuGaSe_2$, $AgGaSe_2$, $AgGaS_2$
- II-IV-V_2 $ZnGeP_2$, $ZnGeAs_2$, $CdGeP_2$, $CdGeAs_2$,

Spin-polarized electron from strained SL

Drescher et al., Appl. Phys. A ***63****, 203 (1996)*

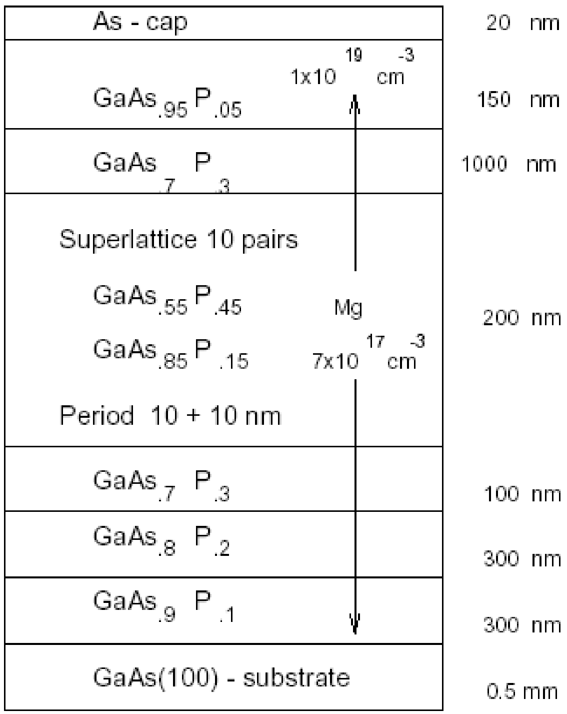

Fig. 1. Structure of strained layer $GaAs_{.95}P_{.05}$ cathode. The different layer thicknesses are not drawn to scale

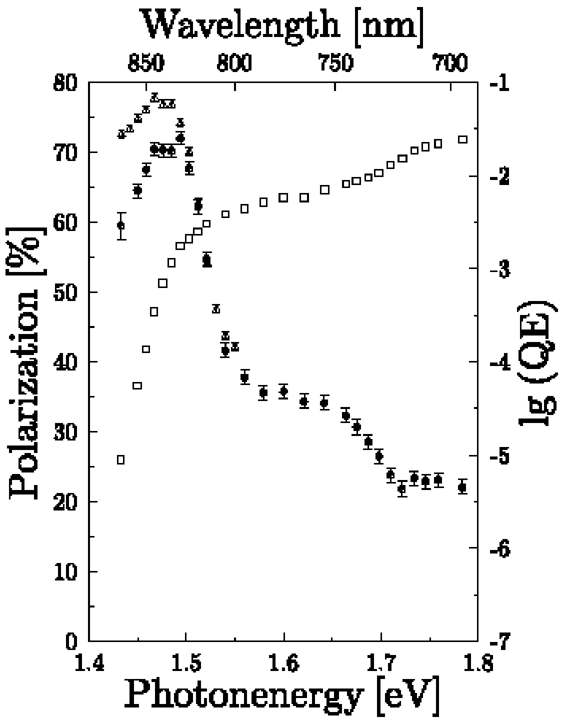

Fig. 3. Photo electron emission from strained $GaAs_{.95}P_{.05}$. Polarization P of emitted electrons and quantum efficiency QE as a function of photon energy of irradiating light. △△△.... ○○○ ....*P*, □□□....*QE*

- Large crystal field splitting requires large strain
- Reduced critical layer thickness lead to low quantum efficiency

Spin-polarized electron from strained SL

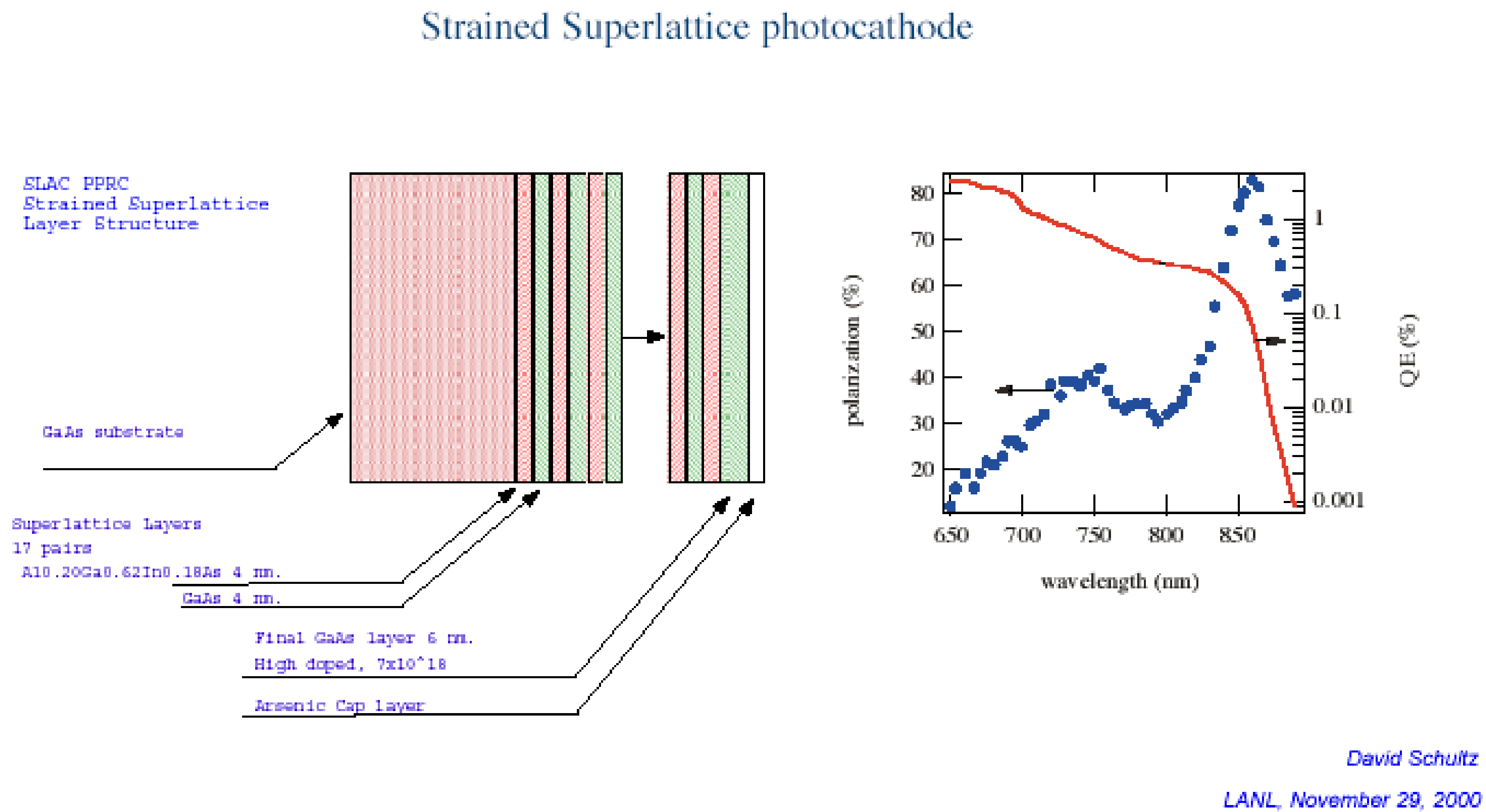

- Large crystal field splitting requires large strain
- Reduced critical layer thickness lead to low quantum efficiency

Spin-polarized electron from ordered alloy

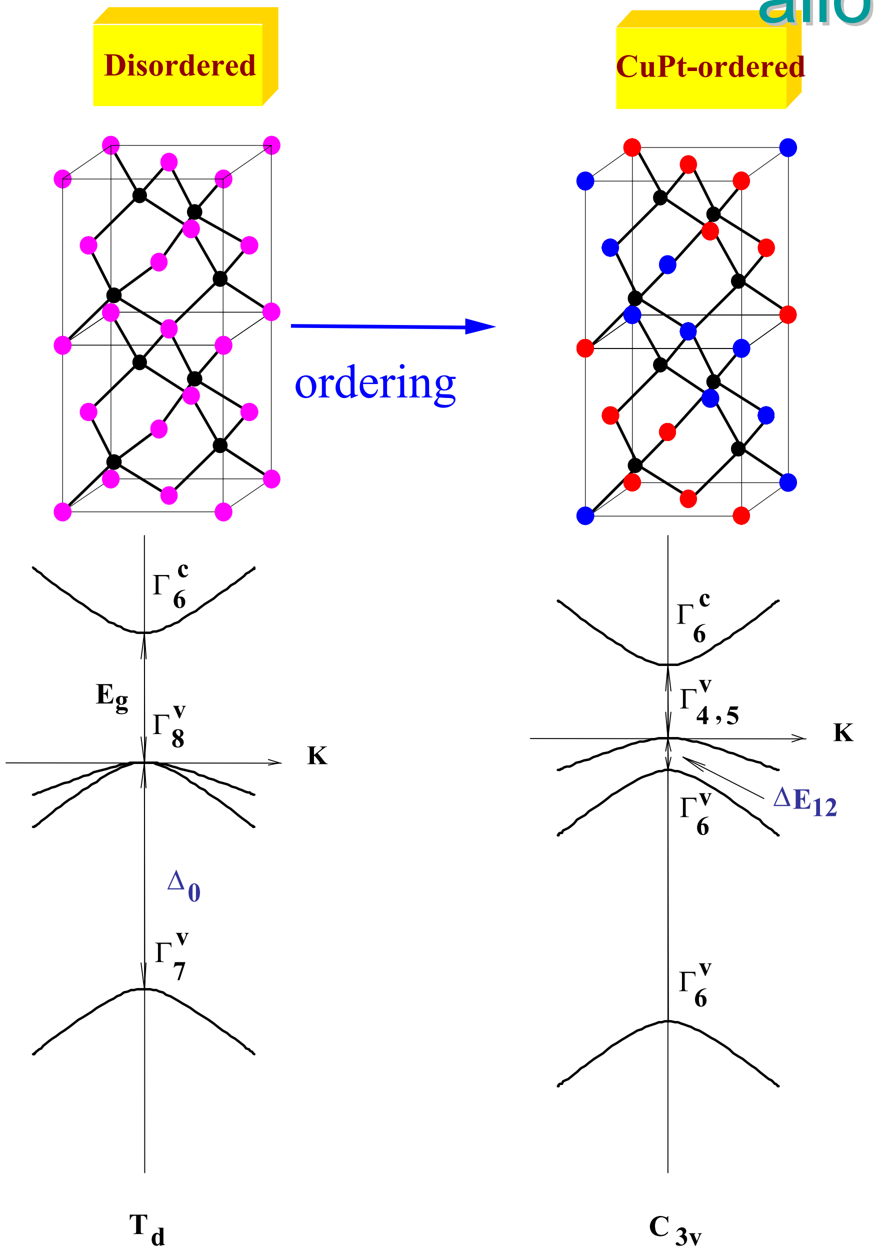

S.-H. Wei,
in Polarized Gas Target and Beams Workshop (1998).

CuPt ordered semiconductor alloy is unstable in the bulk, the degree of ordering and ΔE_{12} are small

Spin-polarized electron from ternary compounds

*L. S. Cardman, Nuclear Phys. A **546**, 317c (1992).*

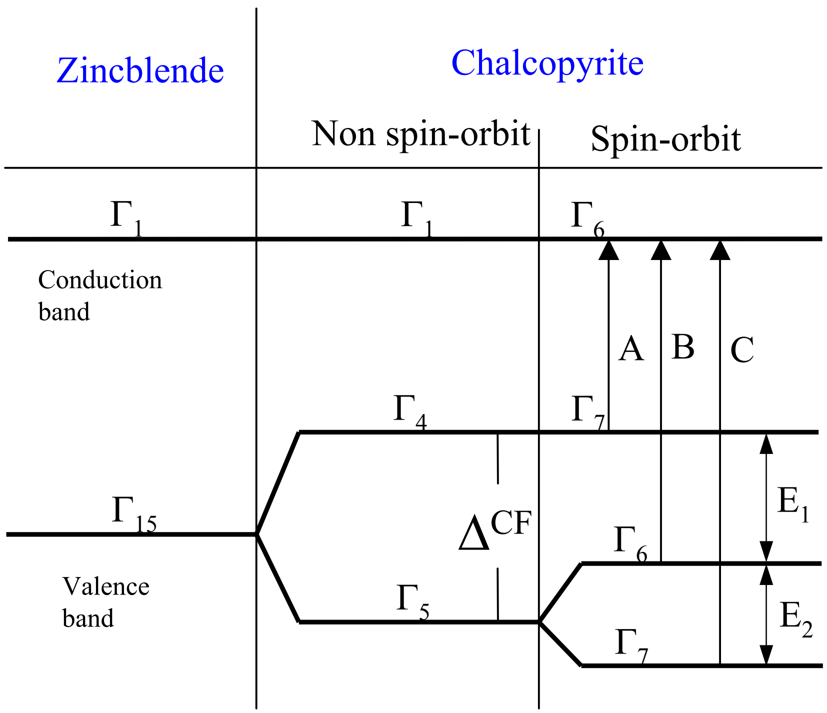

Compounds	a(Å)	c/a	u	E_g (eV)	Δ^{SO} (eV)	Δ^{CF} (eV)
$CuInS_2$	5.523	1.007	0.214	1.53	−0.02	−0.00
$CuInSe_2$	5.784	1.004	0.224	1.04	0.184	−0.02
$CuAlSe_2$	5.602	0.977	0.259	2.67	0.152	−0.16
$CuGaSe_2$	5.614	0.982	0.250	1.68	0.194	−0.12
$CuInTe_2$	6.161	1.003	0.225	1.01	0.598	−0.00
$AgGaS_2$	5.750	0.895	0.291	2.64	−0.02	−0.26
$AgGaSe_2$	5.980	0.910	0.276	1.80	0.252	−0.24

All the chalcopyrites have negative or zero crystal field splitting

Schematic diagram of near-gap optical transition for circularly polarized light

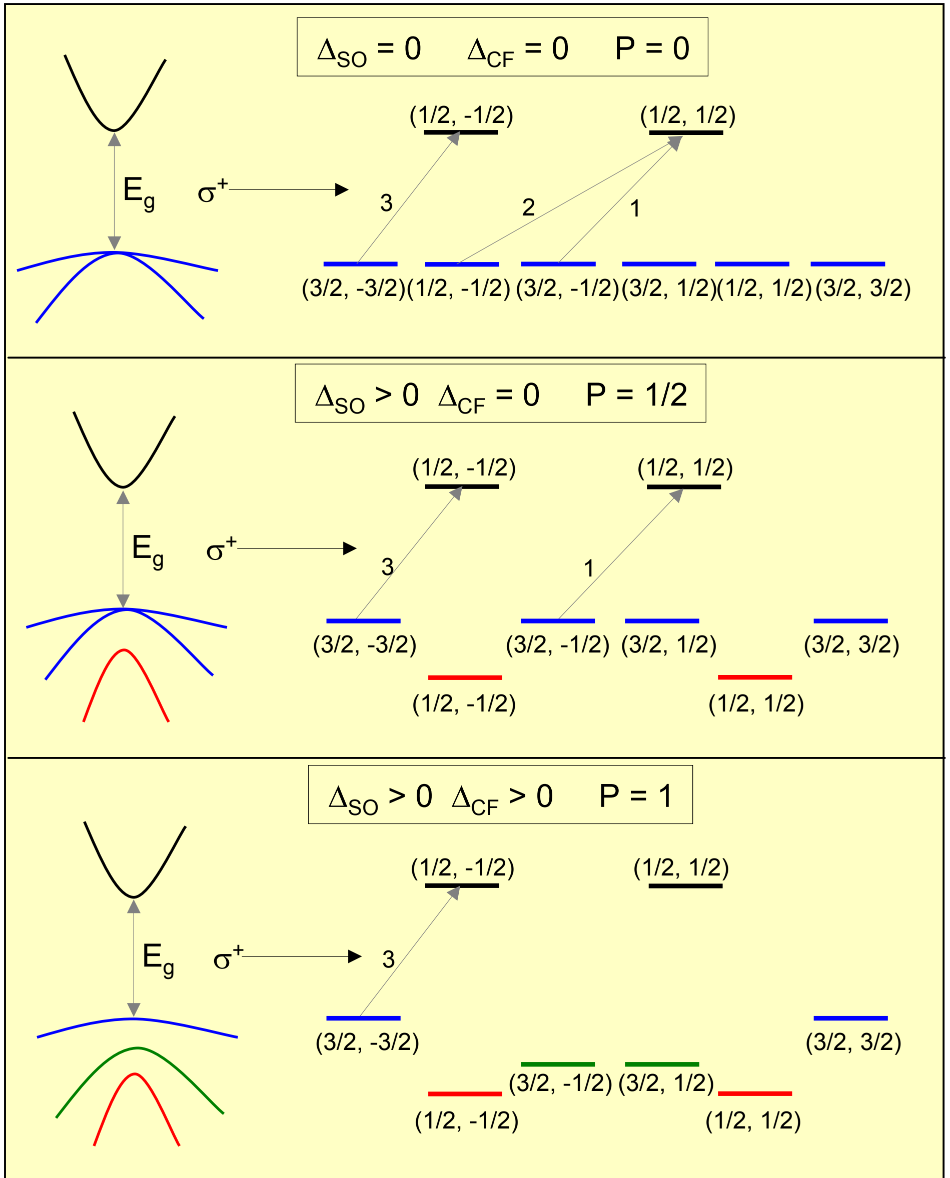

$$P = \frac{|I\downarrow - I\uparrow|}{|I\downarrow + I\uparrow|}$$

$$I = \left|\langle \Psi_f | H_{\text{int}} | \Psi_i \rangle\right|^2$$

$$H_{\text{int}} = X + iY$$ for σ^+ light

Spin-polarized electron from ternary compounds

Compounds	a(Å)	c/a	u	E_g (eV)	Δ^{SO} (eV)	Δ^{CF} (eV)
$CuInS_2$	5.523	1.007	0.214	1.53	−0.02	−0.00
$CuInSe_2$	5.784	1.004	0.224	1.04	0.184	−0.02
$CuAlSe_2$	5.602	0.977	0.259	2.67	0.152	−0.16
$CuGaSe_2$	5.614	0.982	0.250	1.68	0.194	−0.12
$CuInTe_2$	6.161	1.003	0.225	1.01	0.598	−0.00
$AgGaS_2$	5.750	0.895	0.291	2.64	−0.02	−0.26
$AgGaSe_2$	5.980	0.910	0.276	1.80	0.252	−0.24

All the chalcopyrites have negative or zero crystal field splitting

Substantial effort have been made to break GaAs 50% polarization limit

Strained materials

- GaAsP grown on GaAs
- GaAs grown on InGaAs

Reduced critical layer thickness
Poor material quality
Low quantum efficiency

Chalcopyrites

- I-III-VI_2
- II-IV-V_2

Negative or zero crystal field splitting
Low quantum efficiency

Theoretical approach: Density Functional Theory

Rev. Mod. Phys., Vol. 71, No. 5, October 1999

Nobel Lecture: Electronic structure of matter—wave functions and density functionals*

W. Kohn

Department of Physics, University of California, Santa Barbara, California 93106

Hohenberg, P., and W. Kohn, 1964, Phys. Rev. **136**, B864.

Kohn, W., and L. J. Sham, 1965, Phys. Rev. **140**, A1133.

"The total energy, including exchange and correlations, of an electron gas (even in the presence of a static external potential), is a unique functional of the electron density. The minimum value of the total energy functional is the ground-state energy of the system, and the density that yields this minimum value is the exact single-particle ground state density."

many-electron problem ⇔ set of self-consistent one electron equations

Theoretical approach: Density Functional Theory

$$E[\{\psi_i\}]=2\sum_i \int \psi_i \left[-\frac{\hbar^2}{2m}\right]\nabla^2\psi_i \mathbf{d}^3\mathbf{r}+\int V_{\text{ion}}(\mathbf{r})n(\mathbf{r})\mathbf{d}^3\mathbf{r}+\frac{e^2}{2}\int \frac{n(\mathbf{r})n(\mathbf{r}')}{|\mathbf{r}-\mathbf{r}'|}\mathbf{d}^3\mathbf{r}\,\mathbf{d}^3\mathbf{r}'+E_{XC}[n(\mathbf{r})]+E_{\text{ion}}(\{\mathbf{R}_I\})$$

$$n(\mathbf{r})=2\sum_i |\psi_i(\mathbf{r})|^2 \longrightarrow \left[\frac{-\hbar^2}{2m}\nabla^2+V_{\text{ion}}(\mathbf{r})+V_H(\mathbf{r})+V_{XC}(\mathbf{r})\right]\psi_i(\mathbf{r})=\varepsilon_i\psi_i(\mathbf{r})$$

$$V_H(\mathbf{r})=e^2\int \frac{n(\mathbf{r}')}{|\mathbf{r}-\mathbf{r}'|}\mathbf{d}^3\mathbf{r}' \qquad V_{XC}(\mathbf{r})=\frac{\delta E_{XC}[n(\mathbf{r})]}{\delta n(\mathbf{r})}$$

Local Density Approximation: $E_{XC}[n(\mathbf{r})]=\int \varepsilon_{XC}(\mathbf{r})n(\mathbf{r})d^3\mathbf{r}$

$$\frac{\delta E_{XC}[n(\mathbf{r})]}{\delta n(\mathbf{r})}=\frac{\partial[n(\mathbf{r})\varepsilon_{XC}(\mathbf{r})]}{\partial n(\mathbf{r})} \qquad \varepsilon_{XC}(\mathbf{r})=\varepsilon_{XC}^{\text{hom}}[n(\mathbf{r})]$$

M. C. Payne *et al.*: *Ab initio* iterative minimization techniques Rev. Mod. Phys., Vol. 64, No. 4, October 1992

Theoretical approach: Density Functional Theory

Periodic supercells

Bloch's theorem $\psi_i(\mathbf{r}) = \exp[i\mathbf{k}\cdot\mathbf{r}]f_i(\mathbf{r})$ $f_i(\mathbf{r}) = \sum_{\mathbf{G}} c_{i,\mathbf{G}} \exp[i\mathbf{G}\cdot\mathbf{r}]$ $\psi_i(\mathbf{r}) = \sum_{\mathbf{G}} c_{i,\mathbf{k}+\mathbf{G}} \exp[i(\mathbf{k}+\mathbf{G})\cdot\mathbf{r}]$

k-point sampling

Plane-wave basis sets

$$\sum_{\mathbf{G}'} \left[\frac{\hbar^2}{2m} |\mathbf{k}+\mathbf{G}|^2 \delta_{\mathbf{G}\mathbf{G}'} + V_{\mathrm{ion}}(\mathbf{G}-\mathbf{G}') + V_H(\mathbf{G}-\mathbf{G}') + V_{XC}(\mathbf{G}-\mathbf{G}') \right] c_{i,\mathbf{k}+\mathbf{G}'} = \varepsilon_i c_{i,\mathbf{k}+\mathbf{G}}$$

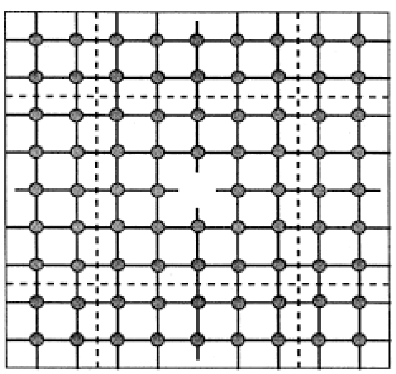

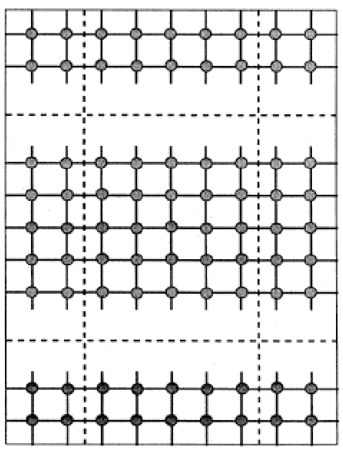

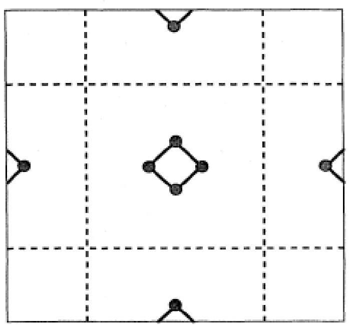

M. C. Payne *et al.*: *Ab initio* iterative minimization techniques Rev. Mod. Phys., Vol. 64, No. 4, October 1992

Self-consistent loop for the calculation of the total energy of a solid

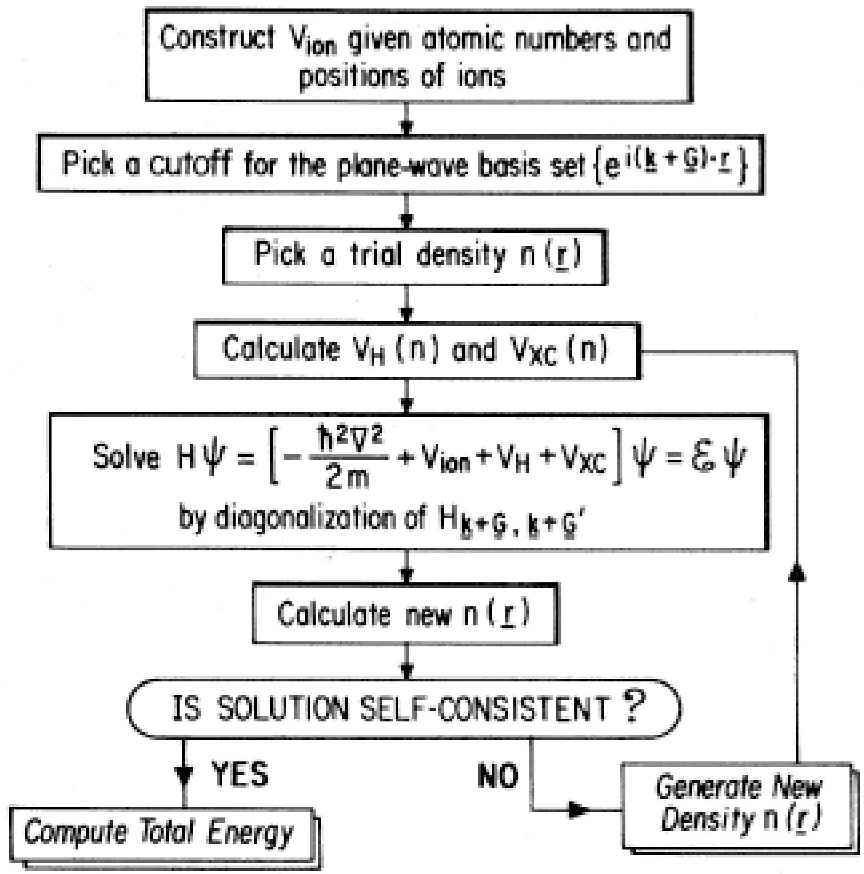

M. C. Payne *et al.*: *Ab initio* iterative minimization techniques Rev. Mod. Phys., Vol. 64, No. 4, October 1992

Theoretical approach: Density Functional Theory - Local Density Approximation

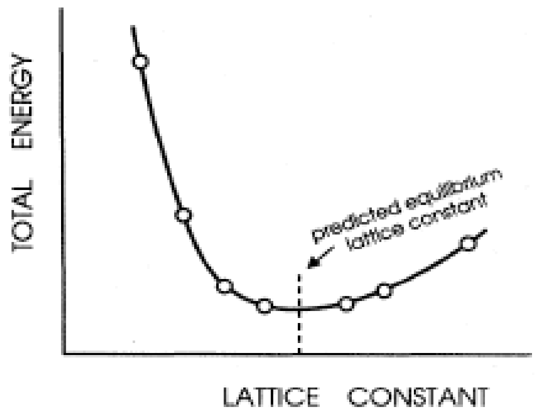

FIG. 1. Theoretical determination of an equilibrium lattice constant. Calculations (open circles) at various possible lattice constants are performed and a smooth function is fitted through the points. The predicted lattice constant is determined by the minimum in the curve.

Equilibrium lattice constant
Elastic constants
Defects
Surfaces
Alloys
High Pressure phases
Earth's core composition

All the chalcopyrites have negative or zero crystal field splitting

Compounds	a(Å)	c/a	u	E_g (eV)	Δ^{SO} (eV)	Δ^{CF} (eV)
$CuInS_2$	5.523	1.007	0.214	1.53	−0.02	−0.00
$CuInSe_2$	5.784	1.004	0.224	1.04	0.184	−0.02
$CuAlSe_2$	5.602	0.977	0.259	2.67	0.152	−0.16
$CuGaSe_2$	5.614	0.982	0.250	1.68	0.194	−0.12
$CuInTe_2$	6.161	1.003	0.225	1.01	0.598	−0.00
$AgGaS_2$	5.750	0.895	0.291	2.64	−0.02	−0.26
$AgGaSe_2$	5.980	0.910	0.276	1.80	0.252	−0.24

CuAu and Chalcopyrite crystal structure

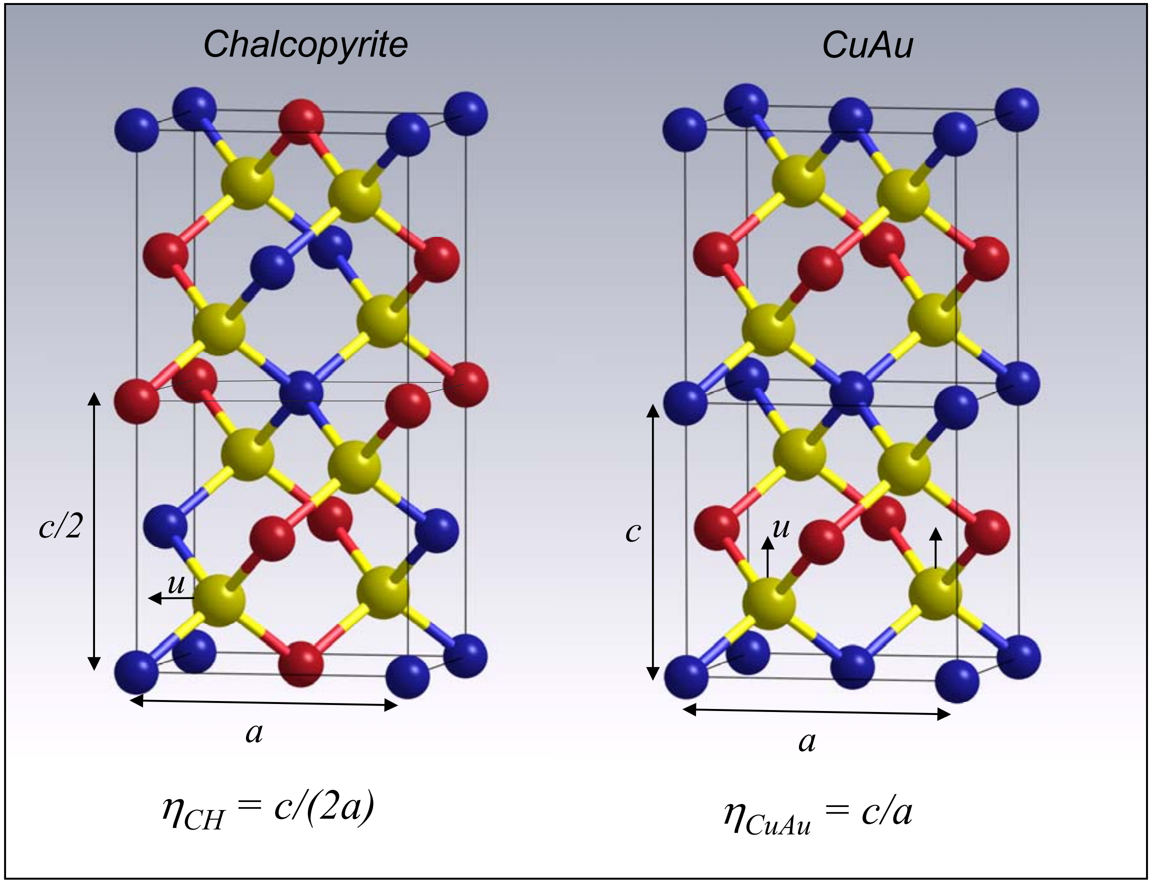

CH: *c* and *u* are in perpendicular directions

CuAu: *c* and *u* are in the same direction

$$\eta_{CuAu} = 2/(3\eta_{CH} - 1)$$

$$\Delta a = a_{CH} - a_{CuAu} \approx 5/6\ (1 - \eta_{CH}) a_{CH}$$

CuAu and Chalcopyrite crystal structure

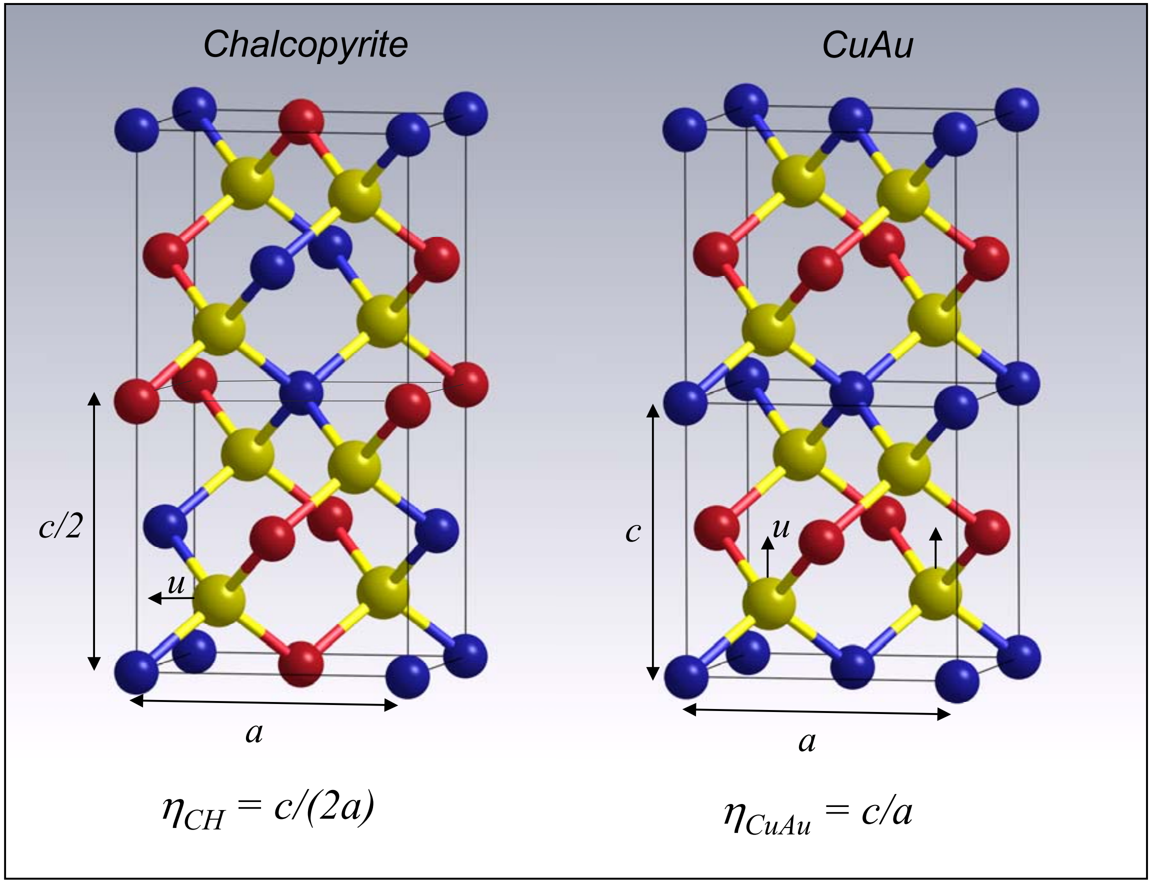

Large η_{CuAu} and large Δa can lead to large positive crystal field splitting and epitaxial stabilization energy

CuAu-like $AgGaSe_2$ and $AgGaS_2$ as possible high-quality SPES

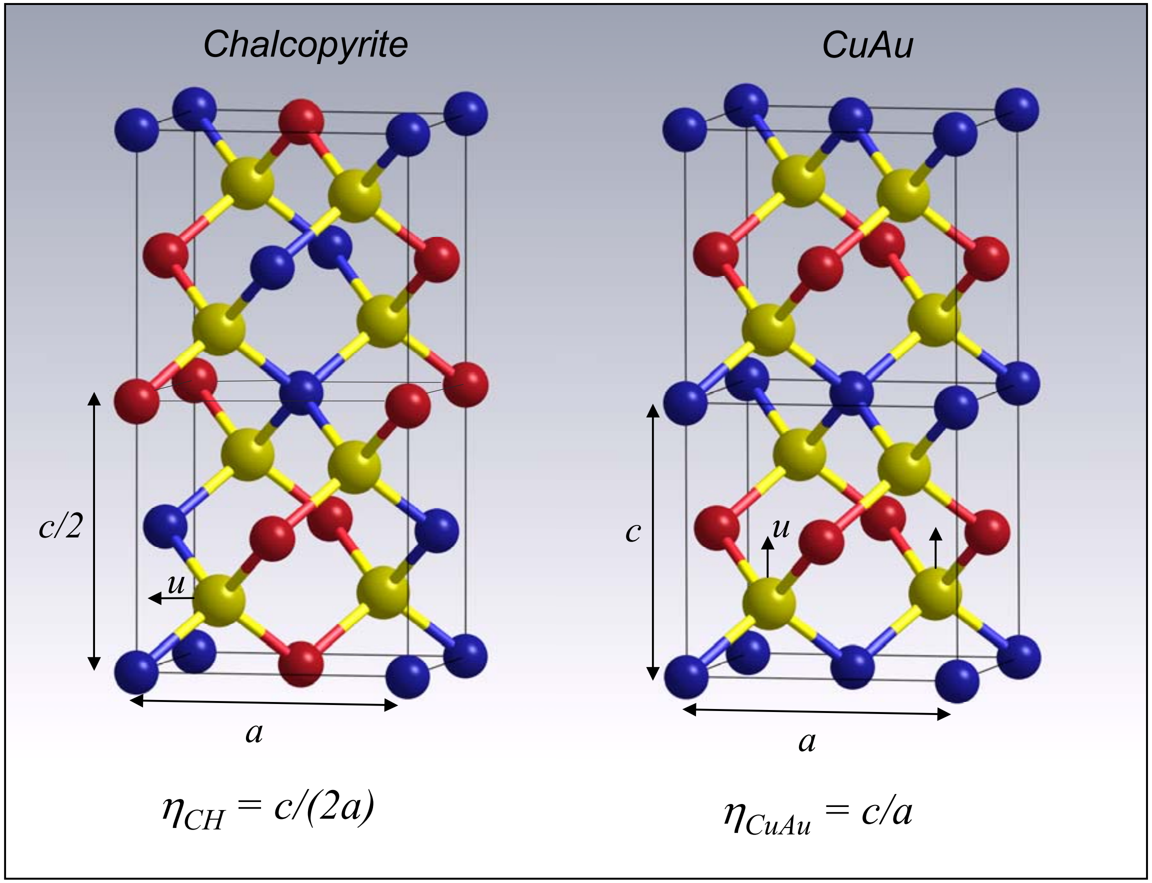

Large η_{CuAu} and large Δa can lead to large positive crystal field splitting and epitaxial stabilization energy

$AgGaSe_2$ and $AgGaS_2$: Total energy vs. lattice constant *a*

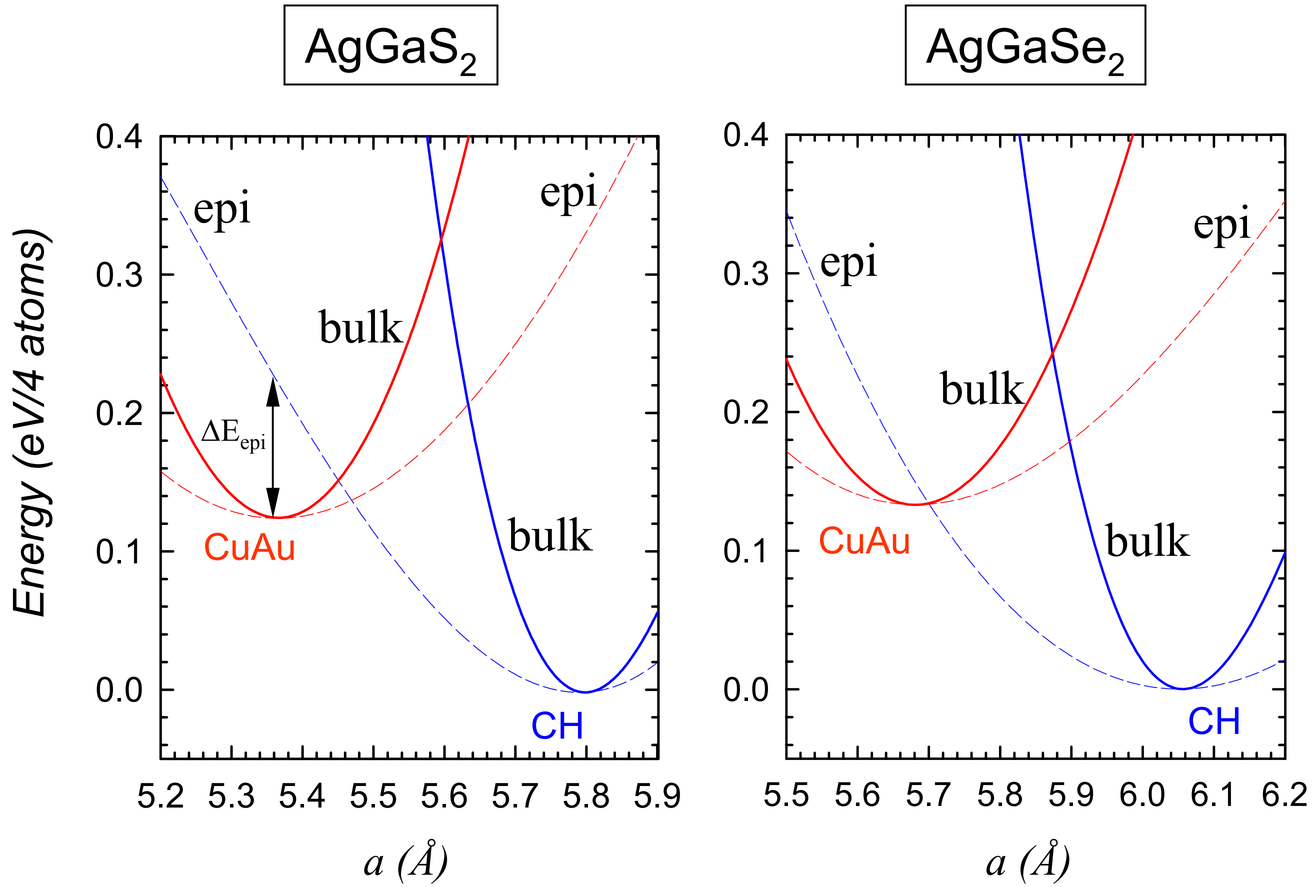

• CuAu-like $AgGaS_2$ has the largest η and largest epitaxial stabilization energy. However, spin-orbit coupling for the sulphide is very small (Δ_{so}=0.02 eV)

• Strain-free CuAu-like $AgGaSe_2$ can be stabilized if it is grown epitaxially on an appropriate substrate (e.g., ZnSe a_0 = 5.66 Å)

$AgGaSe_2$ and $AgGaS_2$: Total energy vs. lattice constant *a*

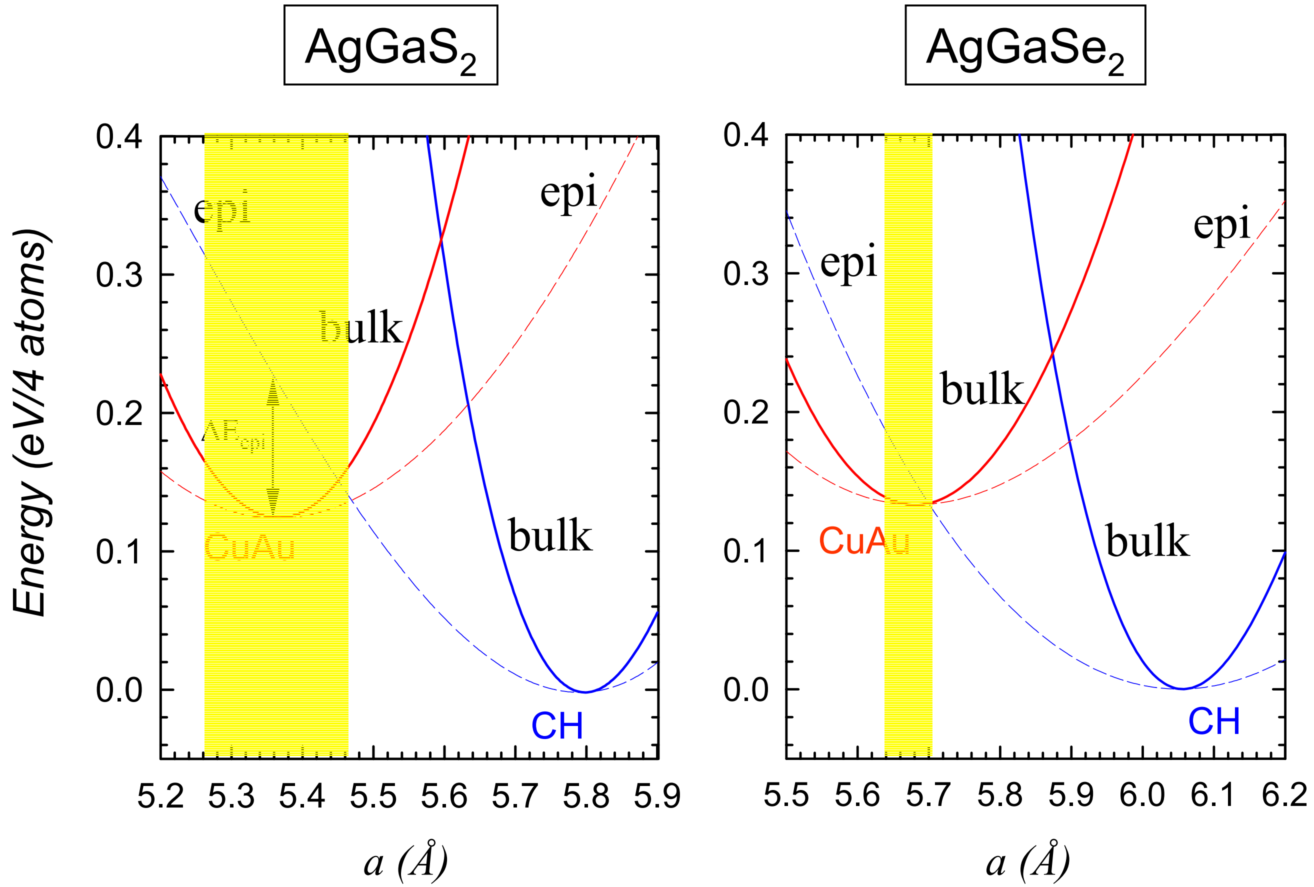

• CuAu-like $AgGaS_2$ has the largest η and largest epitaxial stabilization energy. However, spin-orbit coupling for the sulphide is very small (Δ_{so}=0.02 eV)
• Strain-free CuAu-like $AgGaSe_2$ can be stabilized if it is grown epitaxially on an appropriate substrate (e.g., ZnSe a_0 = 5.66 Å)

$AgGaSe_2$: CuAu vs. Chalcopyrite

Property	CH	Expt.	CuAu
a (Å)	6.054	5.980	5.675
η	0.926	0.910	1.124
u	0.280	0.278	0.274
V/atom (Å^3)	25.68	24.33	25.68
ΔE_g (eV)	0.00	$\cdots$	−0.42
Δ_{CF} (eV)	−0.24	−0.25	0.76
Δ_{SO} (eV)	0.25	0.31	0.21
ΔE_t (eV/4 atoms)	0.000	$\cdots$	0.131
$\Delta E_t^{\dagger}$ (eV/4 atoms)	0.023	$\cdots$	0.000

$AgGaSe_2$ in the CuAu phase has large positive crystal-field and spin-orbit splitting and is epitaxially stable with respect to the chalcopyrite phase

Epitaxially Stabilized CuAu-$AgGaSe_2$ On ZnSe

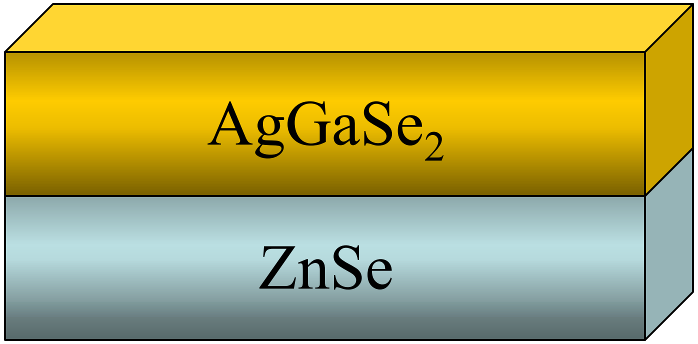

Small lattice mismatch between $AgGaSe_2$ and ZnSe
Common anion avoids the problem of polarity mismatch at the interface
CuAu- $AgGaSe_2$ is not strained

Summary

- $AgGaSe_2$ in CuAu-like phase is a strong candidate for a high-quality SPES material.

  - Direct band gap close to that of GaAs
  - Large spin-orbit splitting
  - Large and positive crystal field splitting

- bulk strain-free films can be obtained if grown under epitaxial conditions with appropriate choice of substrate (ZnSe)

Computational Design of a Material for high-efficiency spin-polarized electron source, A. Janotti & Su-Huai.Wei, Appl. Phys. Lett. **81**, 3957 (2002).